Electronic Supplementary Material (ESI) for Nanoscale.
This journal is © The Royal Society of Chemistry 2019

Supplementary Information

Multifunctional Graphene Oxide-Bacteriophage Based Porous Three-Dimensional Micro-nanocomposites

Paolo Passaretti [1,], Yiwei Sun[2], Inam Khan[3], Kieran Chan[1], Rania Sabo[1], Henry White[4], Timothy R. Dafforn[5] and Pola Goldberg Oppenheimer[1,*]*

[1] School of Chemical Engineering, University of Birmingham, Birmingham, B15 2TT, United Kingdom.
[2] School of Physics and Astronomy, Queen Mary University of London, London, E1 4NS, United Kingdom.
[3] School of Metallurgy and Materials, University of Birmingham, Birmingham, B15 2TT, United Kingdom.
[4] BAE-Systems-Air Sector, Buckingham House, FPC 267, Filton, Bristol, BS34 7QW, United Kingdom.
[5] School of Biosciences, University of Birmingham, Birmingham, B15 2TT, United Kingdom.

*Authors to whom correspondence should be addressed:
e-mail: PXP561@student.bham.ac.uk - Tel.: +44 (0) 778 49 68 145; e-mail: P.GoldbergOppenheimer@bham.ac.uk - Tel: +44 (0) 121 41 45 287

Table of Contents

1. Calibration curves and UV-Vis analyses for components stability

GO and GO-5' serial dilutions in deionised water (DIW) ranging from 0.01 mg mL^{-1} to 0.5 mg mL^{-1} were prepared and analysed with a UV-Vis spectrophotometer. Subsequently, the peak of absorbance at 230 nm was considered to calculate the related calibration curves **(Fig. S1)**.

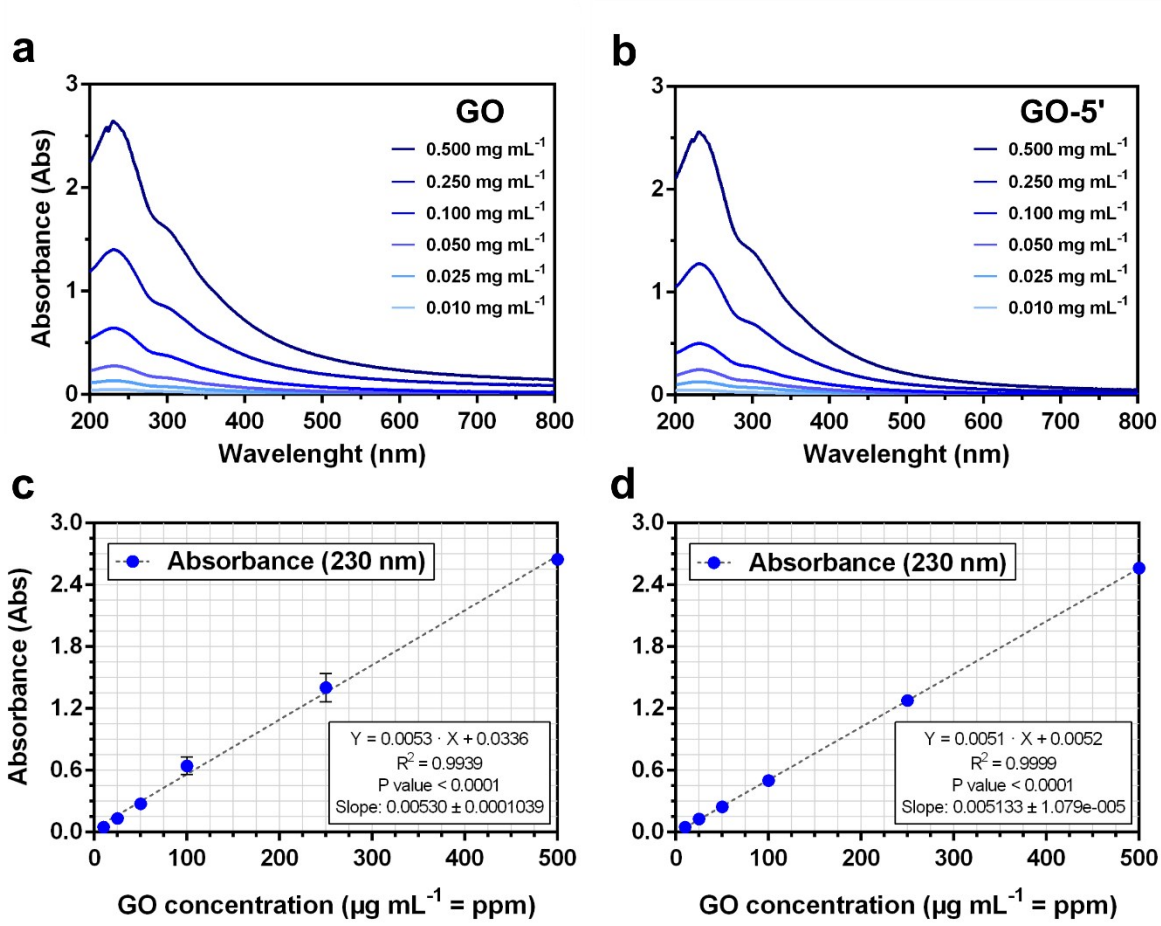

Figure S1 | Graphene oxide calibration curves. (a) GO and **(b)** GO-5' UV-Vis spectra at different concentrations. **(c)** GO and **(d)** GO-5' calibration curves. The spectra acquisition was performed with the same procedure described in the materials and methods section.

The stability of GO, GO-5' and M13 in DIW with representative mean absorbance intensities at specific wavelengths taken in triplicates are shown in the **Table S1** (M13 at 269 nm, GO and GO-5' at 230 nm). Concentrations for M13 and GO were calculated with the Beer-Lambert-Bouguer law and the calibration curves of **Fig. S1f** respectively. The precipitation values refer to the amount of GO or M13, expressed in percentage, that was precipitated after centrifugation, and they were calculated using the difference between the sample and the respective supernatant concentrations.

Table S1. GO, GO-5' and M13 in DIW with absorbance intensities, concentration and percentage of sample precipitated after centrifugation are shown in the table.

	Absorbance (Abs)	***n***	**Concentration (mg mL^{-1})**	**Precipitation (%)**
GO	1.602 ± 0.007	3	0.309 ± 0.001	92.95 ± 0.80
Supernatant	0.113 ± 0.016	3	0.028 ± 0.002	
GO-5'	1.556 ± 0.023	3	0.304 ± 0.004	5.49 ± 1.54
Supernatant	1.471 ± 0.013	3	0.288 ± 0.002	
M13	0.114 ± 0.012	3	0.296 ± 0.025	3.11 ± 6.60
Supernatant	0.110 ± 0.013	3	0.286 ± 0.028	

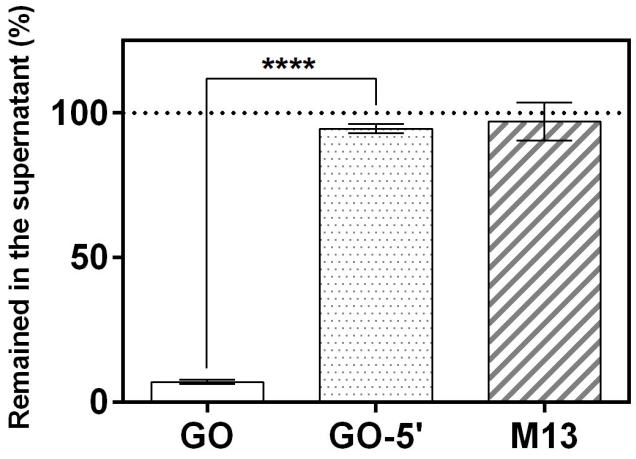

Figure S2 | UV-Vis analysis for components stability. The bars show the amount of GO, GO-5' and M13 left in the supernatant after centrifugation. This bar chart corresponds to the data in **Table S1.** Error bars represent mean ± SD. Statistical significance was assessed performing 2-way ANOVA with post hoc Tukey's multiple comparisons tests ****$p < 0.0001$.

2. Effect of pH on GO and M13 electrostatic charges

Table S2. The pH values of all samples made are shown in the following table.

Media	Sample	pH	*n*
DIW	$GO_{0.3\ mg\ mL^{-1}}$	3.49 ± 0.02	3
	$M13_{0.3\ mg\ mL^{-1}}$	6.97 ± 0.06	3
	$GO\text{-}M13_{03015\text{-}5'}$	3.77 ± 0.02	3
	$GO\text{-}M13_{0303\text{-}5'}$	4.85 ± 0.02	3
	$GO\text{-}M13_{0306\text{-}5'}$	5.72 ± 0.02	3
Citrate Buffer pH 3.5	$GO_{0.3\ mg\ mL^{-1}}$	3.19 ± 0.06	3
	$M13_{0.3\ mg\ mL^{-1}}$	3.44 ± 0.05	3
Citrate Buffer pH 4.9	$GO_{0.3\ mg\ mL^{-1}}$	4.80 ± 0.02	3
	$M13_{0.3\ mg\ mL^{-1}}$	4.95 ± 0.02	3
	$GO\text{-}M13_{03001\text{-}5'}$	4.77 ± 0.03	3
	$GO\text{-}M13_{00103\text{-}5'}$	4.94 ± 0.02	3
	$M13\text{-}GO_{00103\text{-}5'}$	4.80 ± 0.01	3
	$M13\text{-}GO_{03001\text{-}5'}$	4.96 ± 0.03	3
Citrate Buffer pH 6.9	$GO_{0.3\ mg\ mL^{-1}}$	6.71 ± 0.06	3
	$M13_{0.3\ mg\ mL^{-1}}$	7.02 ± 0.06	3
	$GO\text{-}M13_{03001\text{-}5'}$	6.50 ± 0.05	3
	$GO\text{-}M13_{00103\text{-}5'}$	6.85 ± 0.04	3
	$M13\text{-}GO_{00103\text{-}5'}$	6.50 ± 0.06	3
	$M13\text{-}GO_{03001\text{-}5'}$	6.83 ± 0.02	3

Table S3. This table shows the charged amino acids and their corresponding pKa referred to a specific part of the molecule (pKa_1)[2]. Moreover, the alternative pKa_2 and the exposure to the solvent of these amino acids were calculated with PROPKA[3–5]. This software predicts the amino acids pKa considering the presence of the near chemical groups that can alter their standard pKa. These amino acids were divided into three groups based on their position such as the external surface of the phage (white), the middle part of the PVIII protein (light grey) and the internal cavity of the viral capsid (dark grey)[6].

M13 amino acid	Part	Charge	pKa_1	pKa_2	Embedded
A_1	N-terminus	+	9.69	8.62	0%
E_2	Variable group	-	4.25	3.45	0%
D_4	Variable group	-	3.65	3.11	0%
D_5	Variable group	-	3.65	4.02	42%
K_8	Variable group	+	10.53	11.56	0%
E_{20}	Variable group	-	4.25	5.21	25%
Y_{21}	Variable group	-	10.07	14.74	70%
Y_{24}	Variable group	-	10.07	13.14	23%
K_{40}	Variable group	+	10.53	9.67	37%
K_{43}	Variable group	+	10.53	11.17	39%
K_{44}	Variable group	+	10.53	9.91	52%
K_{48}	Variable group	+	10.53	8.16	70%
S_{50}	C-terminus	-	2.21	2.18	53%

3. UV-Vis analysis of *GraPhage13* hydrogel at constant pH and inverted mixing

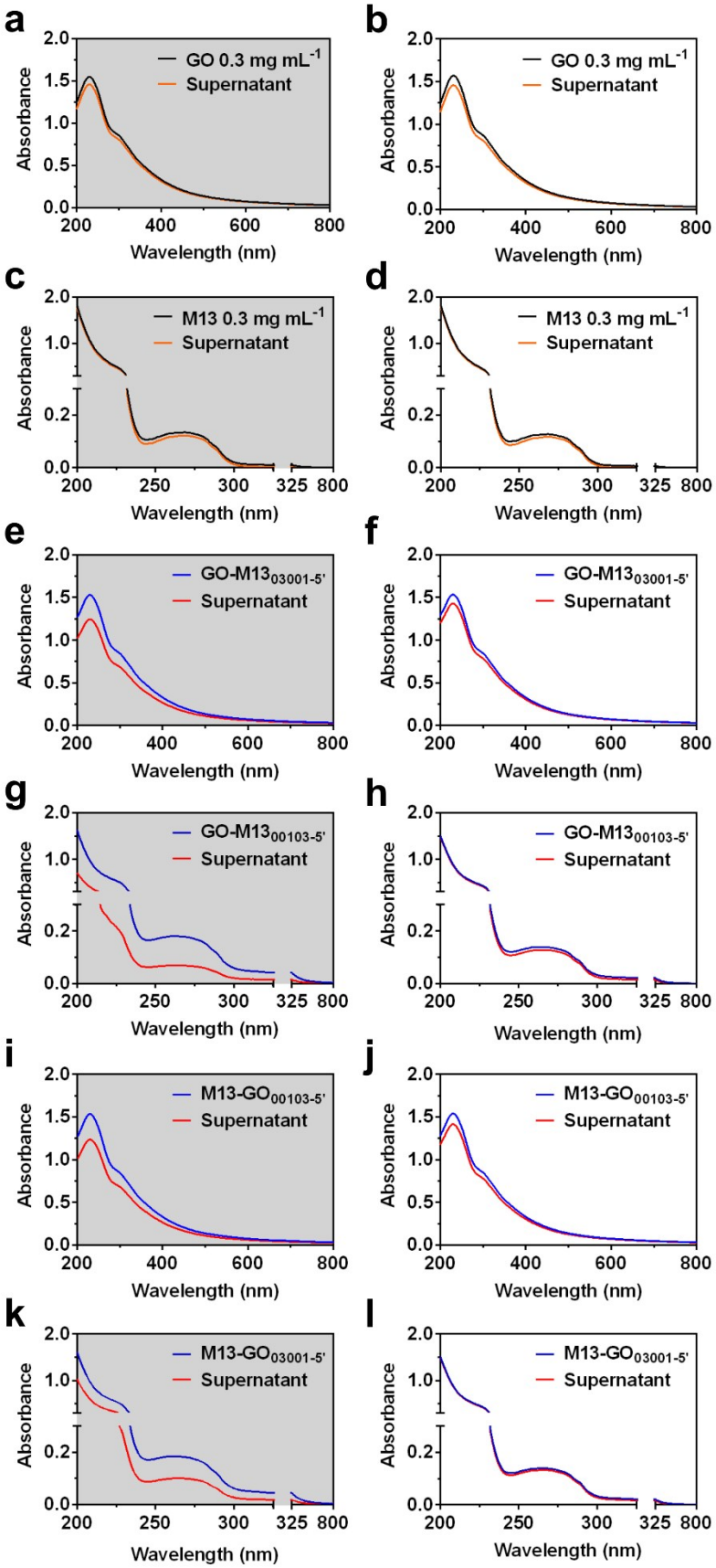

Figure S3 | UV-Vis analysis for the quantitation of the reaction ratio in the formation of GO-M13. This figure shows the UV-Vis spectra of GO, M13 and GO-M13 samples in assembly (grey background) and disassembly pH conditions (white background).

Table S4. This table shows the absorbance values and the respective concentrations of the listed samples referred to **Fig. 4c-e**. The concentrations of starred samples (*) were calculated using the Beer-Lambert-Bouguer law (Absorbance values at 269 nm), while the concentrations of the non-starred once were calculated using the calibration curves of **Fig. S1f** (Absorbance values at 230 nm). The precipitation values refer to the amount of GO or M13, expressed in percentage, that was precipitated after centrifugation, and they were calculated using the difference between the sample and the respective supernatant concentrations, also considering the precipitation percentage of the individual component.

		Absorbance (Abs)	*n*	Concentration (mg mL^{-1})	Precipitation (%)
Citrate Buffer pH 4.9	**GO-5'**	1.548 ± 0.019	3	0.303 ± 0.003	5.84 ± 0.20
	Supernatant	1.458 ± 0.015	3	0.285 ± 0.002	
	***M13**	0.134 ± 0.016	3	0.348 ± 0.035	8.87 ± 3.45
	***Supernatant**	0.122 ± 0.010	3	0.316 ± 0.022	
	GO-M13$_{03001\text{-}5'}$	1.531 ± 0.004	3		13.72 ± 1.53
	Supernatant	1.246 ± 0.029	3	0.244 ± 0.005	
	***GO-M13$_{00103\text{-}5'}$**	0.178 ± 0.005	3		40.20 ± 7.93
	***Supernatant**	0.068 ± 0.013	3	0.177 ± 0.028	
	M13-GO$_{00103\text{-}5'}$	1.537 ± 0.010	3		14.26 ± 1.27
	Supernatant	1.237 ± 0.024	3	0.242 ± 0.004	
	***M13-GO$_{03001\text{-}5'}$**	0.181 ± 0.008	3		16.97 ± 0.89
	***Supernatant**	0.099 ± 0.001	3	0.258 ± 0.003	
Citrate Buffer pH 6.9	**GO-5'**	1.570 ± 0.022	3	0.307 ± 0.004	7.12 ± 0.40
	Supernatant	1.458 ± 0.015	3	0.285 ± 0.002	
	***M13**	0.127 ± 0.013	3	0.330 ± 0.027	7.92 ± 4.28
	***Supernatant**	0.116 ± 0.007	3	0.303 ± 0.015	
	GO-M13$_{03001\text{-}5'}$	1.536 ± 0.022	3		-0.28 ± 1.86
	Supernatant	1.431 ± 0.035	3		
	***GO-M13$_{00103\text{-}5'}$**	0.138 ± 0.007	3		-0.12 ± 5.90
	***Supernatant**	0.127 ± 0.010	3		
	M13-GO$_{00103\text{-}5'}$	1.540 ± 0.023	3		0.99 ± 0.50
	Supernatant	1.415 ± 0.009	3		
	***M13-GO$_{03001\text{-}5'}$**	0.138 ± 0.005	3		-3.02 ± 2.13
	***Supernatant**	0.131 ± 0.004	3		

4. Rheology of *GraPhage13* hydrogel

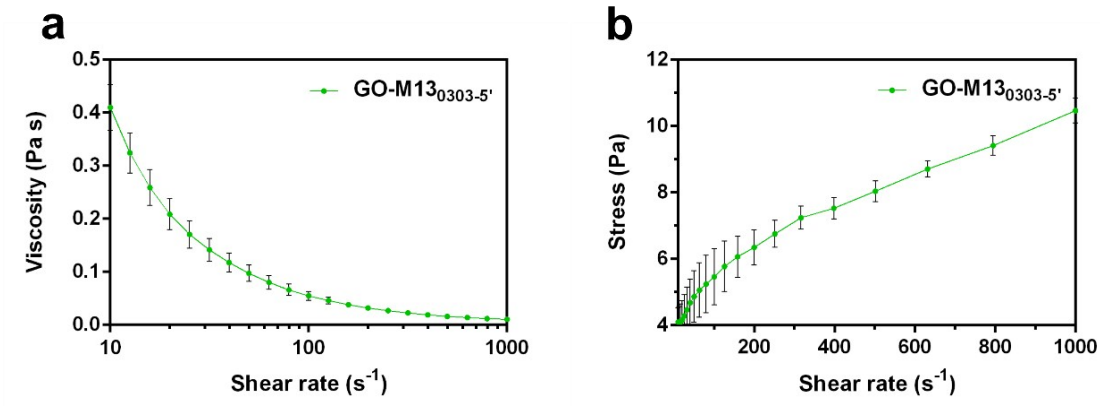

Figure S4 | Rheology. Rheology results showing the shear-thinning behaviour of GPH.

5. Density and surface are measurements

The estimation of GPA density was impossible via a pycnometer or the X-ray micro-CT analyses (data not shown), due to the equipment resolution limits. Given the small dimension and irregular shape of each sponge sample, as well as its extremely low weight, for the calculation of the density, an alternative method was adopted. The latter consisted of demonstrating that the volume of GPA was not varying considerably compared to the volume of the GPH used for its production and therefore, a microbalance was used to weigh the individual sponge and the volume of GPA could be correlated, accordingly. To estimate the change in volume between GPH and GPA, a rotating stage with a fixed camera was used, and each GPH sample was photographed at 0°, 90°, 180° and 270°. Once dried, the fresh GPA was photographed in the same way, and the profile pictures of GPH (red) and GPA (blue) were overlapped **(Fig. S5 and Table S5)**. The comparison of the areas in pixels of GPH and GPA shows that there is a difference of 0.4%, therefore, it is reasonable to assume that GPA and GPH have the same volume (50 mm^3). To measure the weight of an individual sponge, a microbalance of a Dynamic Vapour Sorption apparatus (DVS Advantage - Surface Measurement Systems®) was employed. The average weight of each individual sponge was divided by the average volume giving an ultra-low-density of 8.82 ± 0.03 mg cm^{-3}.

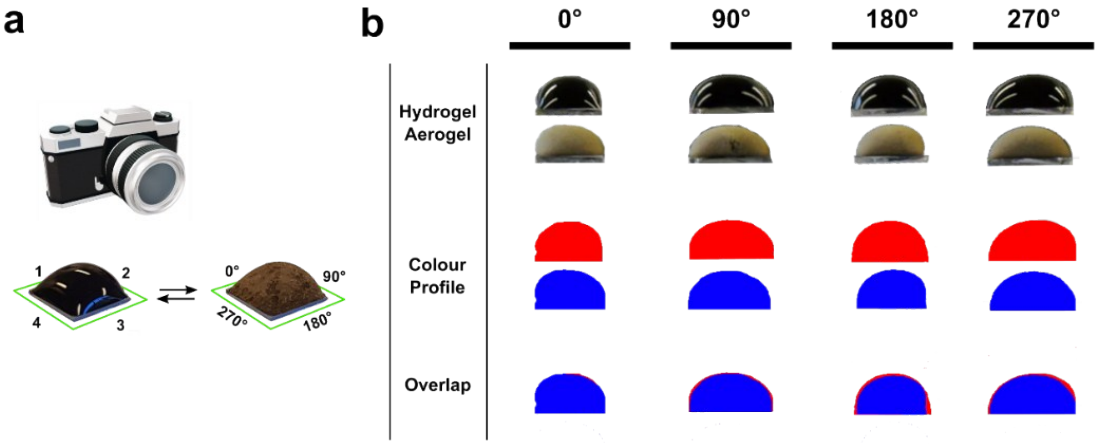

Figure S5 | Density calculation. (a) Schematic representation of the rotating stage used to take pictures of the hydrogels and the corresponding aerogels. **(b)**

Table S5. The area in pixels obtained from the hydrogels and aerogel pictures after the thresholding process.

	Hydrogel area (px)			Aerogel area (px)		
	1	**2**	**3**	**1**	**2**	**3**
0°	6,736	5,564	6,063	6,228	5,723	6,636
90°	5,909	4,890	5,138	5,266	4,444	5,946
180°	6,346	5,783	5,844	6,004	5,557	6,410
270°	5,471	5,207	5,279	5,272	4,584	5,892
Total	68,230 px			67,962 px		
Difference	268 px 0.393%					

Table S6. BET surface area results.

	Samples			Average	SD
	1	2	3		
BET Surface Area	793.48	859.95	1,054.88	902.77	110.93
Single point surface area	276.72	346.80	351.92	325.15	34.31
p/p°	0.273514205	0.273432514	0.27342998	0.27346	0.00004

6. Scanning Electron Microscopy and Energy Dispersive X-ray (SEM/EDX) Spectroscopy

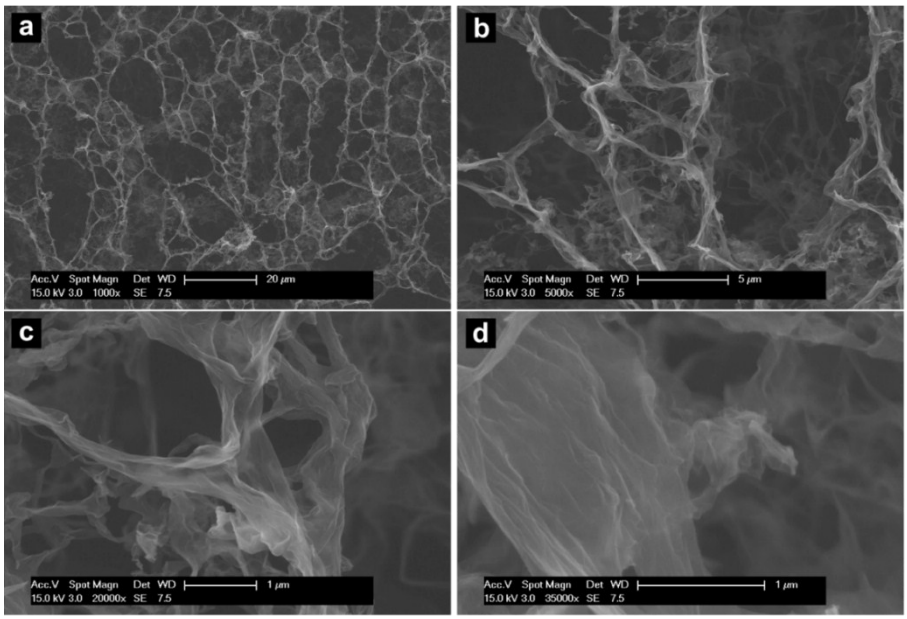

Figure S6 | GO-5' SEM. SEM images of dry GO-5' at different magnifications.

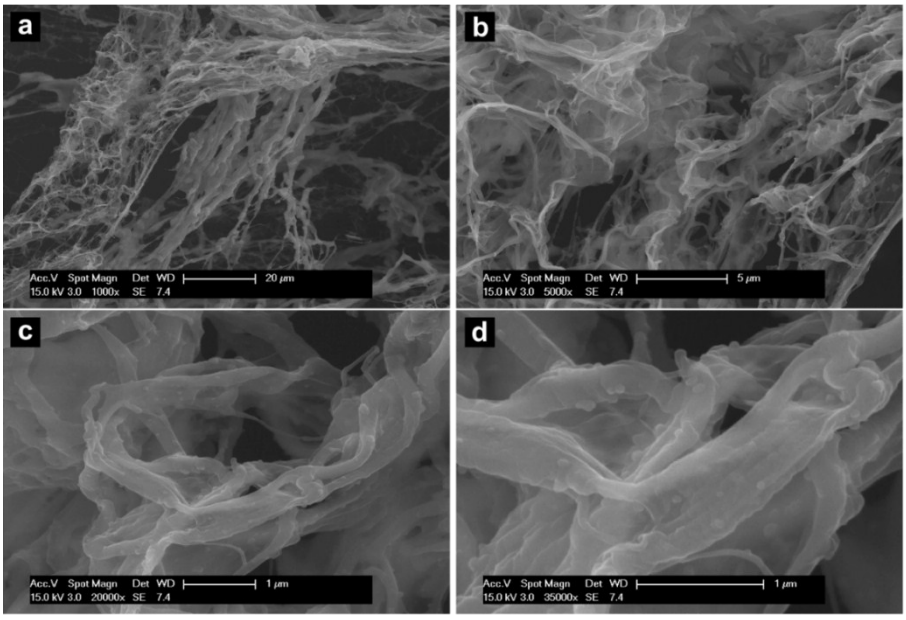

Figure S7 | M13 SEM. SEM images of dry M13 at different magnifications.

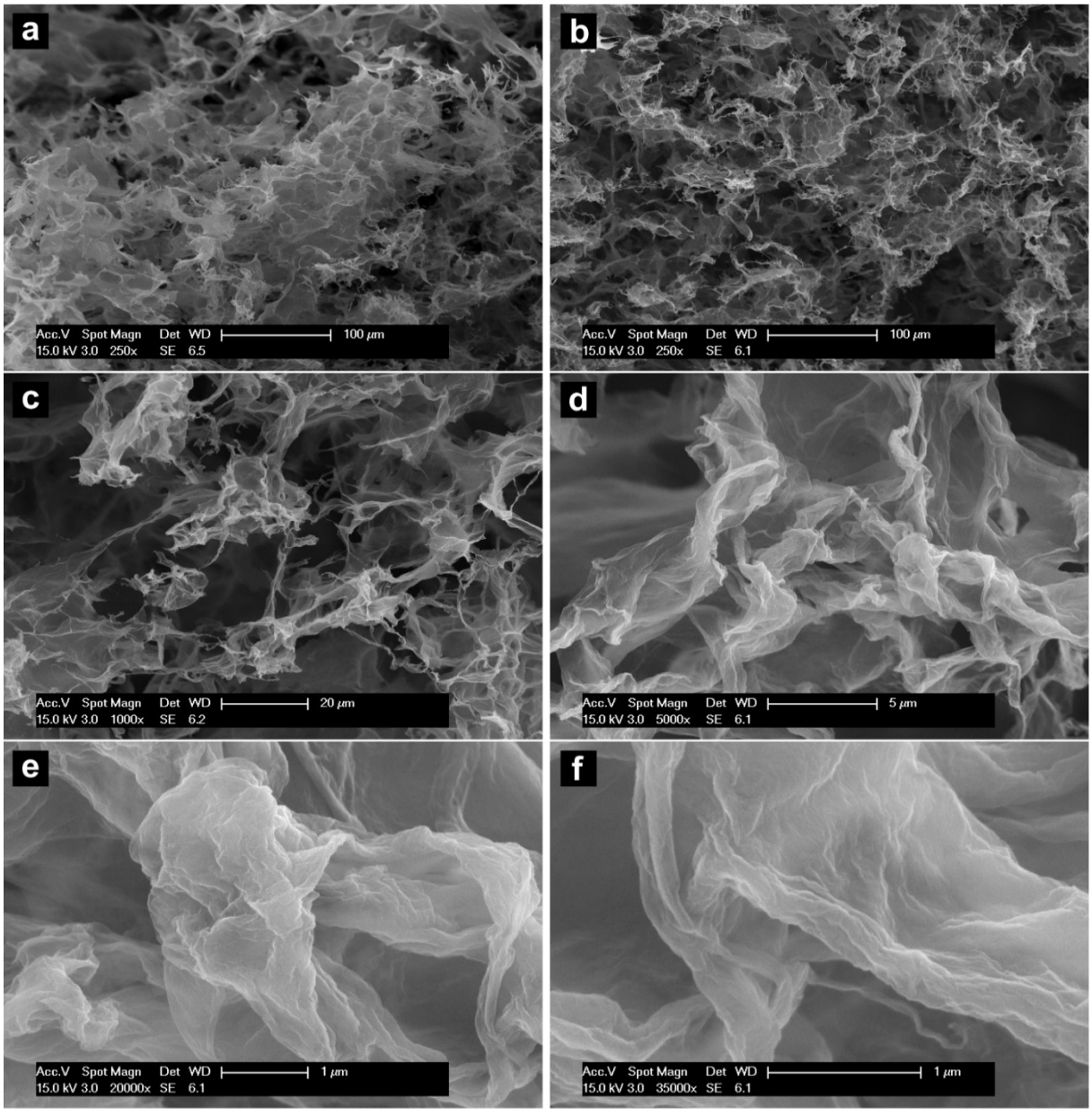

Figure S8 | *GraPhage13* SEM. SEM images of dry GO-M13$_{0303\text{-}5'}$ at different magnifications.

The following SEM/EDX results **(Fig. S9-11 and Tables S7-9)** show GO, M13 and *GraPhage13* respectively. In particular, for each sample, a pink line defines the areas where the EDX spectra were collected (3 spectra per sample). Moreover, the presence of each detected element expressed in percentage, and the average across the repeated acquisition at different locations of the same sample is shown in **Table S7-9**.

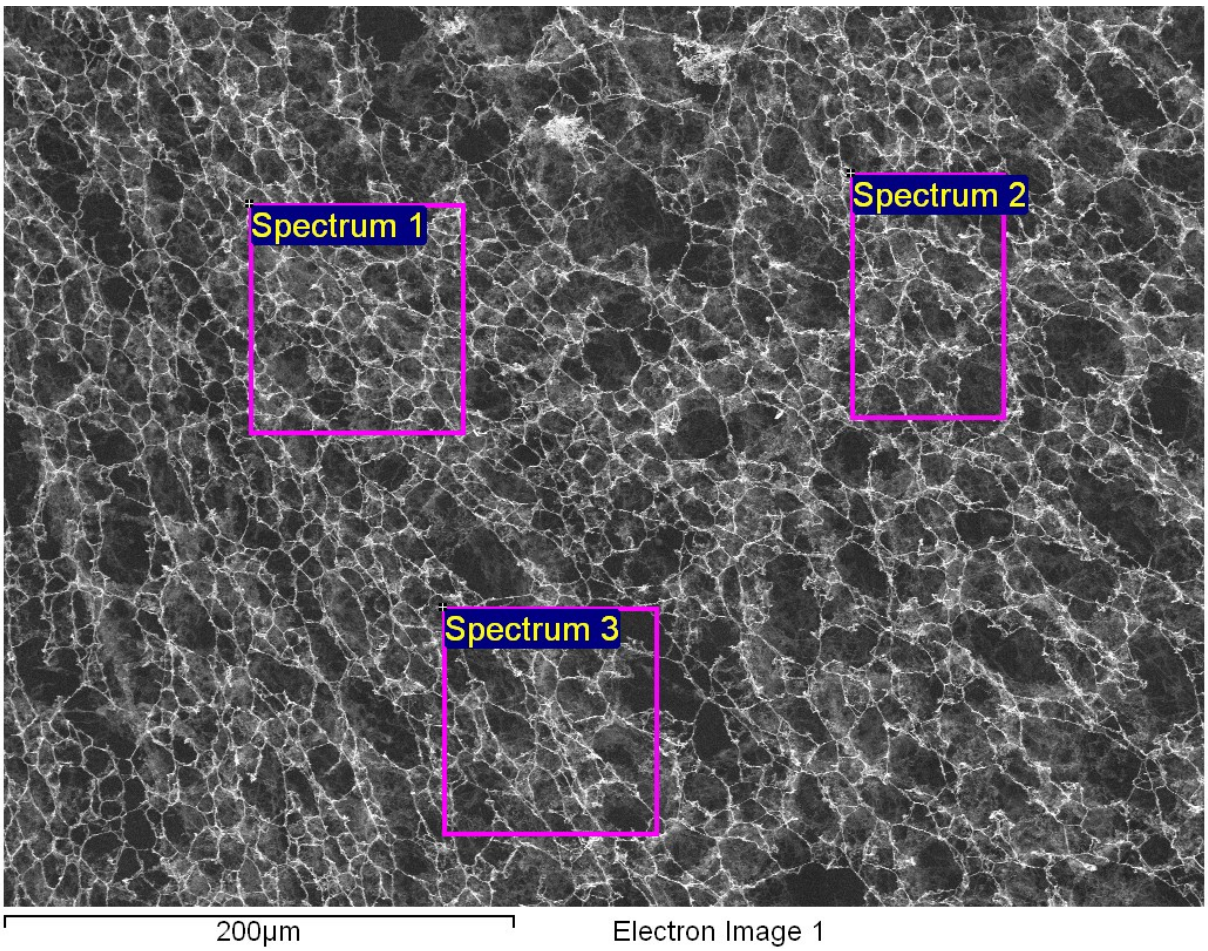

Figure S9 | GO-5' SEM/EDX. SEM images of GO-5' with the areas labelled where the EDX spectra **(Fig. 5)** were collected.

Table S7. GO sample EDX element analysis with results in weight percentage.
GO processing option: All elements analysed (Normalised)

	In stats.	Si	C	O	Total
Spectrum 1	Yes	44.71	45.68	9.61	100.00
Spectrum 2	Yes	48.00	41.70	10.30	100.00
Spectrum 3	Yes	49.03	42.75	8.22	100.00
Mean		47.25	43.38	9.38	100.00
Std. deviation		2.26	2.06	1.06	
Max.		49.03	45.68	10.30	
Min.		44.71	41.70	8.22	

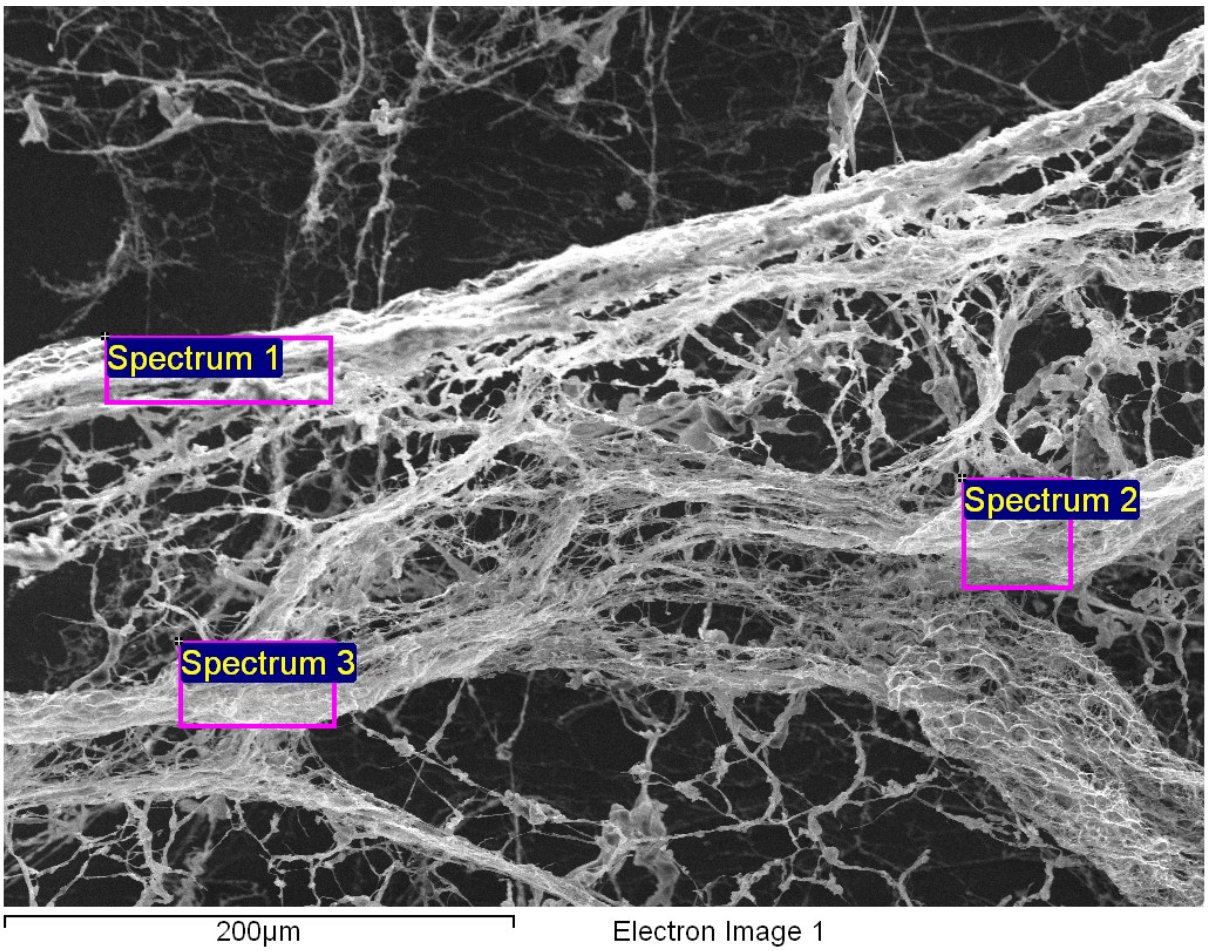

Figure S10 | M13 SEM/EDX. SEM images of M13 with the areas where the EDX spectra **(Fig. 5)** were collected.

Table S8. M13 sample EDX element analysis with results in weight percentage.
M13 processing option: All elements analysed (Normalised)

	In stats.	Si	C	O	N	S	P	Na	Cl	Total
Spectrum 1	Yes	36.41	49.31	8.91	4.09	0.01	0.29	0.43	0.55	100.00
Spectrum 2	Yes	21.42	58.06	13.80	4.79	0.04	0.19	0.69	1.01	100.00
Spectrum 3	Yes	28.25	54.30	10.56	5.46	0.05	0.31	0.39	0.68	100.00
Mean		28.69	53.89	11.09	4.78	0.03	0.26	0.50	0.75	100.00
Std. deviation		7.50	4.39	2.49	0.69	0.02	0.06	0.16	0.24	
Max.		36.41	58.06	13.80	5.46	0.05	0.31	0.69	1.01	
Min.		21.42	49.31	8.91	4.09	0.01	0.19	0.39	0.55	

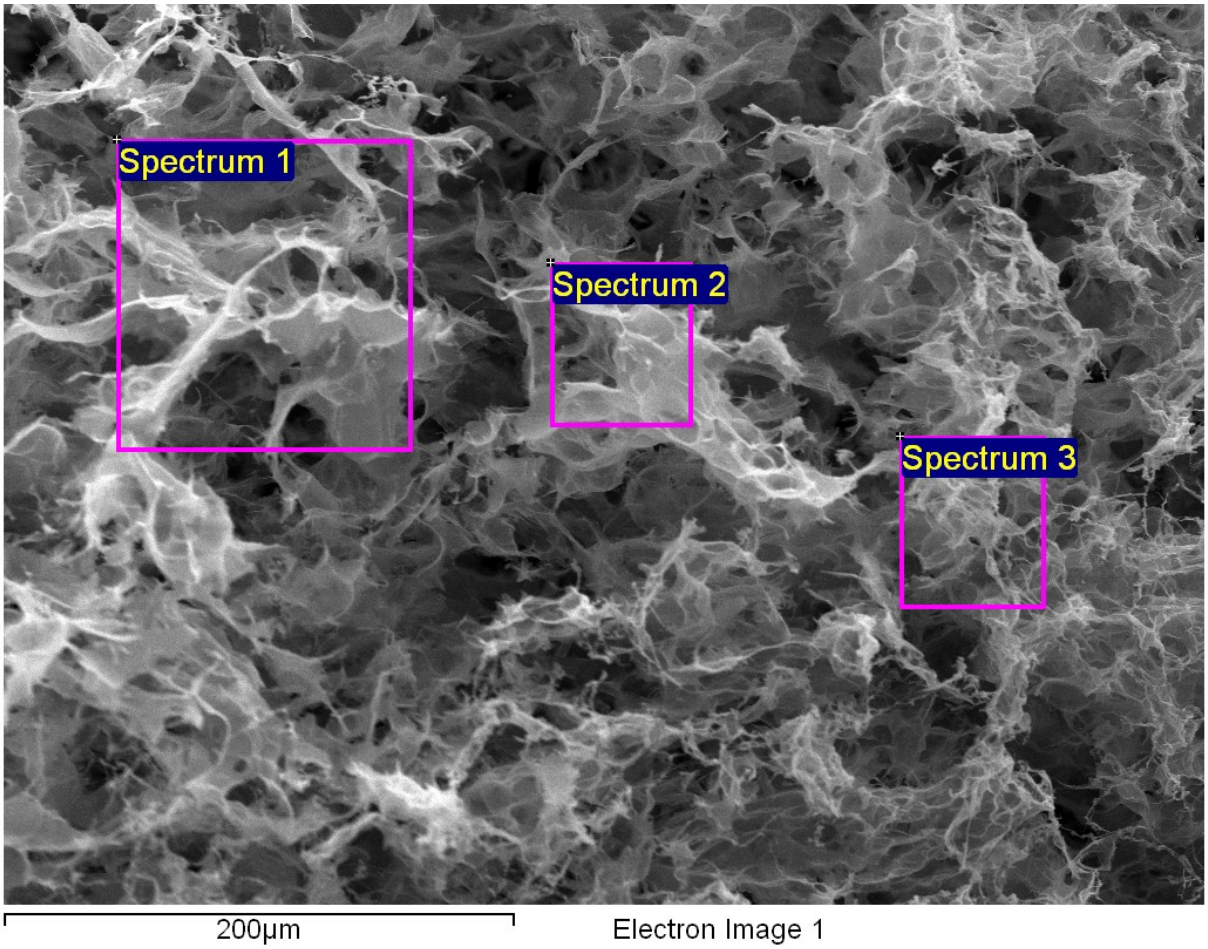

Figure S11 | *GraPhage13* SEM/EDX. SEM images of GO-M13$_{0303\text{-}5'}$ with the areas where the EDX spectra **(Fig. 5)** were collected.

Table S9. GO-M13$_{0303\text{-}5'}$ sample EDX element analysis with results in weight percentage.
GO-M13$_{0303\text{-}5'}$ processing option: All elements analysed (Normalised)

	In stats.	Si	C	O	N	S	P	Na	Cl	Total
Spectrum 1	Yes	2.95	66.25	27.59	1.63	0.29	0.63	0.35	0.30	100.00
Spectrum 2	Yes	2.18	58.89	29.03	8.76	0.20	0.23	0.40	0.31	100.00
Spectrum 3	Yes	1.23	60.92	29.79	6.72	0.26	0.28	0.40	0.40	100.00
Mean		2.12	62.02	28.80	5.70	0.25	0.38	0.38	0.34	100.00
Std. deviation		0.86	3.80	1.12	3.67	0.05	0.22	0.03	0.06	
Max.		2.95	66.25	29.79	8.76	0.29	4.19	0.35	0.40	
Min.		1.23	58.89	27.59	1.63	0.20	1.42	0.40	0.30	

7. Raman spectroscopy and analyses of *GraPhage13* aerogel

We demonstrate the fitting procedure to get the best fit that we presented. We subtracted the spectrum by a straight line to make it flat. We fitted the spectrum by Lorentzians for peaks and Fourier series for the background. We compared the BIC and residuals from fittings using various numbers of Lorentzians and Fourier terms and obtained the optimal. Two examples of the best fit of the spectra of M13 at 633 and 785 nm were presented in **Fig. 6b, c**.

7.1. Fitting results of the Raman spectra collected at 633 nm

Table S10 summarises the frequencies of the optimal fits for each of the four spectra shown in **Fig. 6a** along with the corresponding widths and amplitudes, P for position, W for width and A for the integrated area.

Table S10. The position, width and amplitude of the Lorentzians from the best fits of the spectra of the GO, M13, GO-M13$_{PC}$ sample and GO-M13$_{0303\text{-}5'}$ at 633 nm are shown. The fitted position corresponds to the Raman shift. P1 denotes the position of the Lorentzian with the lowest frequency. The width and amplitude of the Lorentzian are labelled corresponding to the positions. W1 and A1 denote the width and amplitude of the peak with the position P1.

	GO	M13	GO-M13$_{PC}$	GO-M13$_{0303\text{-}5'}$
P1 (cm^{-1})	1,292.2	1,309.2	1,339.1	1,335.2
P2	1,337.7	1,450.4	1,585.2	1,575.8
P3	1,586.5	1,592.6		1,606.2
P4		1,652.6		
W1 (cm^{-1})	6.8	47.8	61.5	60.9
W2	60.9	20.5	37.9	34.4
W3	39.6	41.3		20.0
W4		11.0		
A1 (arb. unit)	2.3E+4	5.4E+4	7.1E+5	9.6E+6
A2	1.6E+6	3.7E+4	3.6E+5	3.3E+6
A3	8.3E+5	1.9E+4		1.4E+6
A4		1.7E+4		

At the excitation wavelength of 633 nm, the fitted two peaks in **Table S10** of GO-M13$_{PC}$ arise from the GO, as their position, width and intensity ratios are in a good agreement with the second and third fitted peak in the GO. The two peaks of the GO-M13$_{PC}$ spectrum correspond to the unmodified sp^2 and sp^3 bonds of the GO[7].

The value of P1 in the sponge is very close to P2 in the GO. W1 in the sponge is the same as W2 in the GO. P1 in the sponge is likely from the sp^3 of GO. Similarly for the second peak observed for the sponge which can be, therefore, attributed to the unmodified sp^2 of GO. Furthermore, since the intensity ratio of the sp^3 to sp^2 peaks is ~2:1 in the GO, the ratio in the sponge should be 2:1, but it is not until we assign not only the second but also the third fitted peak of the sponge in **Table S10** to the sp^2. The third peak is blue-shifted by 20 wavenumbers from the sp^2 of GO. Therefore, in the assembled GO-M13 sponge approximately 30% of sp^2 bond from GO, is stiffened by ~2%. These results solidify the proposed sponge-formation mechanism, in which interaction between the two components is critical.

The values of the coefficients of the Fourier series from the best fits for each spectrum are listed in **Table S11**.

Table S11. S[*i*] denotes the *i*th coefficients of *sin* term in the Fourier series, and C[*i*] denotes the *i*th *cos* term.

633 nm	GO	M13	GO-M13$_{PC}$	GO-M13$_{0303\text{-}5'}$
S[1]	-166	0.29	-78	-893
S[2]	469	-2.78	177	2,339
S[3]	-292	8.49	-127	-1,222
S[4]	292	1.12	129	830
S[5]		14.4		1,375
C[0]	-97	-2.17	-41	-402
C[1]	289	-1.49	130	2,550
C[2]	-98	-6.71	-36	-5
C[3]	94	-0.57	1	545
C[4]	99	-2.48	24	438
C[5]		-17.0		-240

7.2. Fitting results of the Raman spectra collected at 785 nm

The fitting results of the spectra obtained at 785 nm are shown in **Table S12**. More Raman modes are in resonance, and therefore appear to be seen. The situation is more complicated, but the key conclusion stands that in the sponge, 30% of the sp^2 bonds from the GO and/or M13 are modified to a certain stiffness.

Table S12. The positions, width and amplitude of the Lorentzians from the best fits of the spectra of the GO, M13, GO-M13$_{PC}$ and GO-M13$_{0303\text{-}5'}$ at 785 nm are shown. The rule of labelling is the same as that for 633 nm.

	GO	M13	GO-M13$_{PC}$	GO-M13$_{0303\text{-}5'}$
P1 (cm^{-1})	1,329.0	1,302.7	1,323.8	1,279.9
P2	1,492.5	1,341.4	1,490.4	1,314.4
P3	1,589.1	1,451.2	1,611.2	1,368.5
P4		1,608.9	1,620.7	1,510.6
P5		1,655.1		1,582.6
P6				1,606.4
W1 (cm^{-1})	60.6	29.5	63.8	36.0
W2	90.9	26.1	65.2	62.4
W3	44.4	20.4	54.9	50.3
W4		27.2	54.6	69.9
W5		13.0		29.2
W6				17.6
A1 (arb.unit)	2.4E+6	6.0E+3	4.4E+6	5.3E+5
A2	1.9E+6	3.3E+3	6.9E+5	8.5E+6
A3	1.6E+6	6.7E+3	7.2E+6	1.6E+6
A4		1.5E+3	5.5E+6	2.3E+6
A5		3.1E+3		1.8E+6
A6				6.4E+5

The values of the coefficients of the Fourier series from the best fits for each spectrum are listed in **Table S13**.

Table S13. S[*i*] denotes the *i*th coefficients of *sin* term in the Fourier series, and C[*i*] indicates the *i*th *cos* term.

785 nm	GO	M13	GO-M13$_{PC}$	GO-M13$_{0303\text{-}5'}$
S[1]	221	0.327	678	1,103
S[2]	297	0.562	-106	-666
S[3]	237	0.665	-313	-790
S[4]	335	1.320	174	438
S[5]	318	2.070		-225
S[6]				-419
C[0]	-119	-0.249	-245	-407
C[1]	-263	-0.715	45	289
C[2]	-170	-0.644	496	1,006
C[3]	-53	-0.629	-190	-532
C[4]	111	-0.139	235	24
C[5]	-154	-1.040		-165
C[6]				-204

References

1. *Konkena, B. & Vasudevan, S.* **Understanding aqueous dispersibility of graphene oxide and reduced graphene oxide through pKa measurements**. *J. Phys. Chem. Lett.* 3, 867–872 (2012).

2. *Lide, D. R.* **CRC Handbook of Chemistry and Physics 90th Edition**. *J. Am. Chem. Soc.* 131, 12862–12862 (2009).

3. *Li, H., Robertson, A. D. & Jensen, J. H.* **Very fast empirical prediction and rationalization of protein pKa values**. *Proteins Struct. Funct. Bioinforma.* 61, 704–721 (2005).

4. *Bas, D. C., Rogers, D. M. & Jensen, J. H.* **Very fast prediction and rationalization of pKa values for protein-ligand complexes**. *Proteins Struct. Funct. Bioinforma.* 73, 765–783 (2008).

5. *Olsson, M. H. M., Søndergaard, C. R., Rostkowski, M. & Jensen, J. H.* **PROPKA3 Consistent treatment of internal and surface residues in empirical pKa predictions**. *J. Chem. Theory Comput.* 7, 525–537 (2011).

6. *van Wezenbeek, P. M. G. F., Hulsebos, T. J. M. & Schoenmakers, J. G. G.* **Nucleotide sequence of the filamentous bacteriophage M13 DNA genome: comparison with phage fd**. *Gene* 11, 129–148 (1980).

7. *Tuinstra, F. & Koenig, J. L.* **Raman spectrum of graphite**. *J. Chem. Phys.* 53, 1126–1130 (1970).